Linking Reduction in Measured MIMO Capacity with Dominant-Wave Propagation

Markus Herdin[1], Hüseyin Özcelik[1], Helmut Hofstetter[2] and Ernst Bonek[1,2]
{markus.herdin,hueseyin.oezcelik}@tuwien.ac.at, hofstetter@ftw.at,
ernst.bonek@tuwien.ac.at
[1]Institut für Nachrichtentechnik und Hochfrequenztechnik
Technische Universität Wien
Gußhausstrasse 25/389, A-1040 Wien, Austria
[2]FTW, Forschungszentrum Telekommunikation Wien
Tech Gate Vienna, Donau-City-Strasse 1/3. Stock, A-1220 Wien, Austria

Abstract

We measured the channel capacity of an 8×8 multiple-input multiple-output system in a rich-scattering office scenario at 5.2GHz. We found that there exist remarkable receive positions and directions within a single office, where a strong reduction in MIMO capacity can be observed. Another reduction is due to different transmit array alignment. Investigating the directions-of-departure and direction-of-arrival, we show that these effects are related to dominant-wave propagation.

1 Introduction

The position dependence of the MIMO capacity is an important parameter for system design. In [1] and [2] it was shown that the measured MIMO capacity in indoor scenarios is mainly dependent on the receive SNR but not on the receive position. Normalizing the measured channel matrices to a *fixed* average receive SNR, it appears that the different receive (RX) positions and directions show surprisingly low variation in the MIMO capacity. This is not the case if we include the pathloss. Nevertheless, there are specific RX positions and directions where a significant reduction in the measured MIMO capacity appears. Also, the alignment of the transmit array has an influence on MIMO capacity. In this paper we will investigate why this is the case and show how this reduction is related to dominant-wave propagation.

2 Measurement

2.1 Measurement Setup

For the measurements, we used the wideband vector channel sounder RUSK ATM [3] with a measurement bandwidth of 120MHz at a center frequency of 5.2GHz. At the receive side, a $\lambda/2$ spaced 8-element uniform linear patch array (ULA) with two additional dummy elements was used. Each single patch antenna had a 3dB beamwidth of 120° and was consecutively multiplexed to a single receiver chain. At the transmit (TX) side, a monopole antenna was mounted on a 2D positioning table where the position was controlled by the channel sounder by means of two stepping motors. The monopole transmit antenna was moved to 20 (x) × 10 (y) positions on a rectangular grid with $\lambda/2$ spacing forming a virtual TX matrix *without* mutual coupling.

For each TX position the channel sounder measured 128 temporal snapshots of the frequency dependent transfer function between the TX monopole and all RX antennas. 193 equidistant frequency samples of the channel coefficients were taken within the measurement bandwidth of 120 MHz. Altogether, this resulted in a $(128\times193\times8\times200)$ 4-dimensional complex channel transfer matrix containing the channel coefficients for each snapshot, frequency, RX and TX position. Since the measurement of the whole 4-dimensional channel transfer matrix took about 10 minutes, we took the measurements at night to ensure stationarity.

2.2 Scenario

The measurements were carried out in the offices of the Institute of Communications and Radio Frequency Engineering at the Vienna University of Technology. A number of different office rooms were measured, always with the TX antenna positioned on the same place on the corridor. For our evaluation we took only the measurements of a single room with the RX antenna placed on 8 different positions. For each RX po-

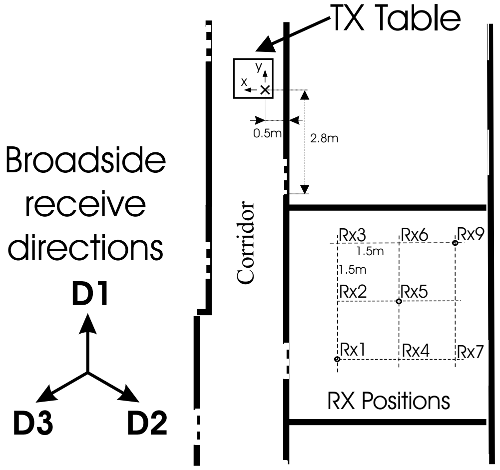

Figure 1: Floor plan of the corridor and office rooms

sition we measured using three different broadside directions of the RX ULA (D1, D2 and D3), angularly spaced by 120°. The room was amply furnished with wooden and metal furniture and plants, without line of sight to the TX (Figure 1) and during the measurement the door to this room was open.

3 Data Evaluation

3.1 Generating Different Channel Realizations

From the measured 4-dimensional MIMO channel matrix we created different realizations of an 8x8 MIMO systems. We grouped 8 adjacent TX positions to a virtual 8-element TX ULA and moved this virtual array over all possible TX positions. We did this for both an x-aligned and a y-aligned virtual TX ULA (Figure 2) to consider also the effect of different TX antenna alignments on the MIMO capacity. In case of x-alignment we have 13 possible movements in x- and 10 possible movements in y-direction, in total 130 different spatial realizations. The y-aligned system leads to 20 x- and 3 y-movements, i.e. 60 spatial realizations.

Using all 193 frequency realizations, we have in the first case 25.090 and in the second case 11.580 spatial and frequency realizations. This gives us enough realizations for an accurate estimate of the mean MIMO capacity.

3.2 MIMO Capacity and Normalization

The MIMO capacity for each spatial and frequency realization was calculated by [4]

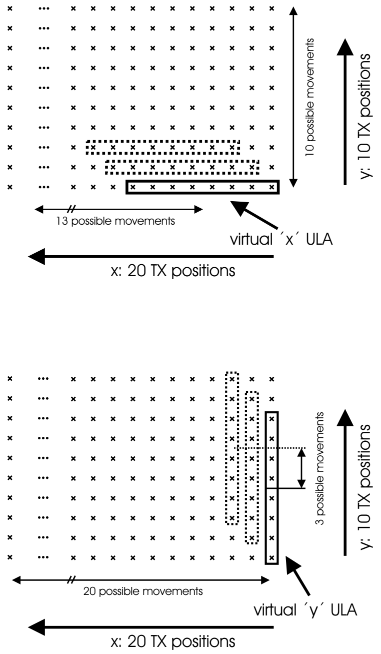

Figure 2: Generation of different MIMO channel realizations for x-axis (top) and y-axis (bottom) aligned TX antenna

$$C = \log_2 \det \left(\mathbf{I_8} + \frac{\rho}{n} \mathbf{H}\mathbf{H}^H \right) \tag{1}$$

where $\mathbf{I}_8$ denotes the 8x8 identity matrix, $n = 8$ the number of transmit antennas, $\mathbf{H}$ the MIMO channel matrix and ρ the average receive SNR (for a normalized channel matrix). The superscript H denotes hermitian transposition. This gives the capacity when the channel is not known at the transmitter.

Since the measured MIMO matrices include the path-loss we had to do a proper normalization. For each system and each RX position, this was done by setting the equivalent SISO pathloss as defined by

$$\frac{1}{n^2} \sum_{i=1}^{n} \sum_{j=1}^{n} |h_{ij}|^2 \tag{2}$$

to 0dB on average over all spatial and frequency realizations. Here h_{ij} is the corresponding MIMO channel matrix element. For all evaluations in this paper we fixed the average receive SNR ρ to 10dB.

Using the normalized MIMO channel realizations, we calculated the average MIMO capacity for each RX position and direction and for both TX antenna alignments.

3.3 DOD and DOA estimation

To link the calculated average MIMO capacities to wave propagation, we estimated the directions of departure (DODs) and directions of arrival (DOAs) with Capon's beamformer [5]. Although the resolution of this beamformer is very limited due to the small number of antennas, it turns out that it is sufficient to estimate the dominant directions reliably. Using the Capon angular spectrum defined as

$$P(\theta) = \frac{1}{\mathbf{a}^H(\theta)\hat{\mathbf{R}}^{-1}\mathbf{a}(\theta)} \tag{3}$$

we stepped in one-degree steps through the DODs and DOAs to find the peaks. Here $\mathbf{a}(\theta)$ is the array steering vector for the given direction θ and $\hat{\mathbf{R}}$ is the estimated spatial covariance matrix.

For an accurate estimate of the covariance matrix we used the different frequencies as realizations and applied spatial smoothing and forward/backward averaging. In case of the DOD estimation four and in case of the DOA estimation two subarrays were used for spatial smoothing.

The DOD estimation was done for both TX ULA alignments. For x-alignment we used 20-element TX ULAs and did the DOD estimation for the 10 possible y-movements and for all 8 receive antennas resulting in 80 realizations of the Capon's DOD spectrum. Correspondingly, for y-alignment we used 10-element ULAs resulting in $20 \cdot 8$ (x-movement and RX antenna) realizations of the Capon's DOA spectrum. The different DOD and DOA spectrum realizations gives us the possibility to check if the DOD and DOA estimates are reliable or not, since they should not change over a small area like the TX table or within the RX antenna array.

4 Results

4.1 MIMO capacity for x-aligned TX array

Figure 3 shows the average MIMO capacity for each receive position and direction when using an x-aligned TX ULA. As mentioned, the average receive SNR for each position and direction is set to 10dB. Except for RX position 3 and 5, the capacity is nearly independent of both the direction and position. Whether we look at the open door at position Rx1 and direction D3 or at the corner at position Rx7 and direction D2, the capacity does not change significantly. This means, that even from directions where dominating multipath components are expected, we still have sufficient scattering to reach high MIMO capacities.

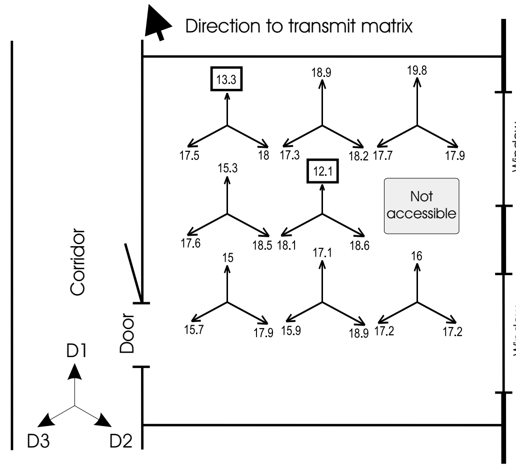

Figure 3: Average MIMO Capacity in bit/s/Hz for each receive position and direction with TX ULA in x direction

This does not hold for position Rx3 and Rx5. The reason for this can be found in the estimated DOAs depicted in figure 4. There, Capon's DOA spectrum for receive position Rx5 and direction D1 versus the TX position is shown. As can be seen, there exists a strong component coming from about $-35°$. Further the DOA does not change with TX position, which means on one hand that the DOA estimation is reliable and on the other hand the multipath scenario does not change significantly over the whole TX table.

In contrast to this, the DOA spectrum for receive position Rx1 direction D2, shows a widely spread angular spectrum. As a consequence we reach very high MIMO capacity.

4.2 MIMO capacity for y-aligned TX array

To investigate the effect of rotated TX arrays on the MIMO capacity, we also considered a y-aligned TX ULA. The resulting capacities for each RX position and direction are plotted in figure 5.

Compared to the results from the x-aligned TX ULA, the capacity is generally lower. Still it is more or less independent of the receive position and direction.

The reason for lower capacity values for y-aligned TX ULA is again dominant-wave propagation. Figure 6 (top) depicts the Capon DOD spectrum for x-aligned TX ULA. Note that here a 20-element virtual ULA was used for the estimation. As mentioned before, the possible y-movements of the TX array and all 8 RX antennas were used to create different realizations

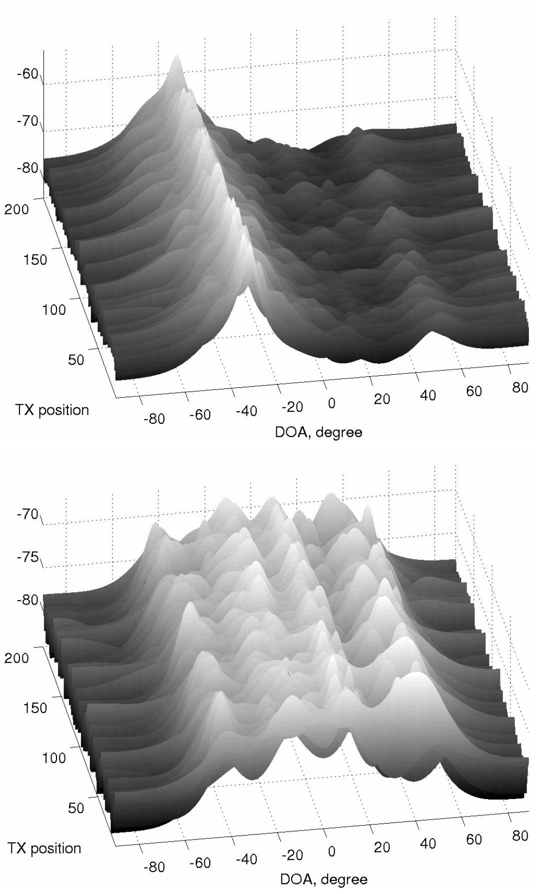

Figure 4: Capon DOA spectrum for receive position Rx5, direction D1 (top), receive position Rx1, direction D2 using an x-aligned TX ULA vs transmit antenna position

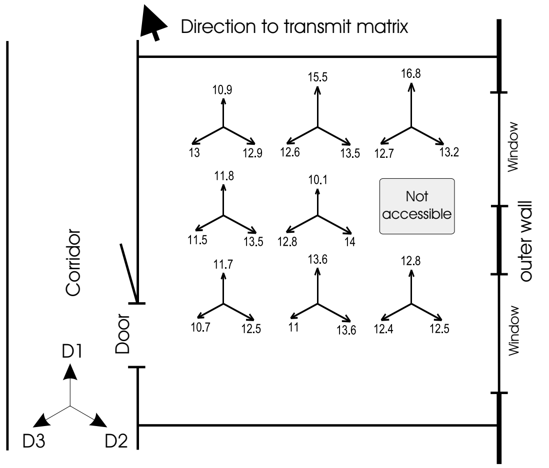

Figure 5: Average MIMO Capacity in bit/s/Hz for each receive position and direction with TX ULA in y direction

of the DOD spectrum. In figure 6 (bottom) the corresponding DOD spectrum for y-aligned TX ULA is shown. Here, we can only make use of a 10-element TX ULA and therefore we get worse resolution. Here, we used the different x-movements of the virtual ULA and all 8 receive antennas to create different DOD spectrum realizations.

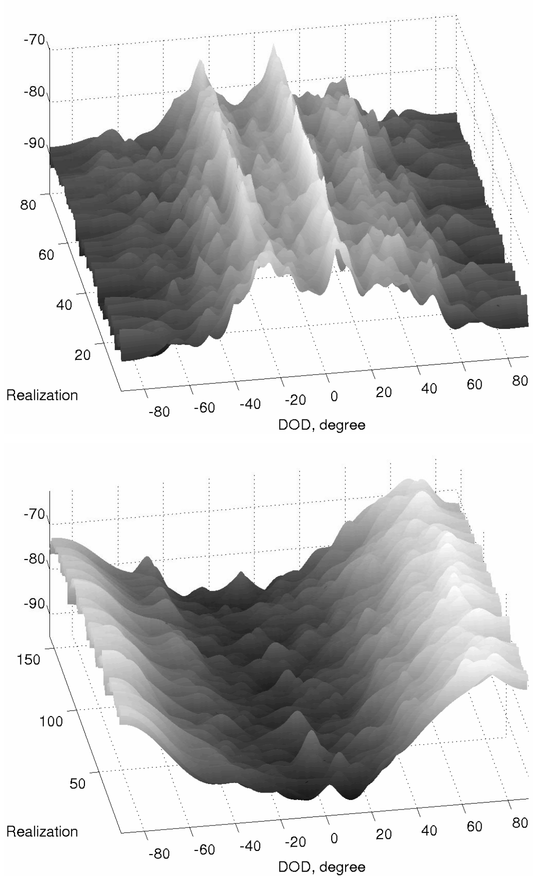

Figure 6: Capon DOD spectrum for receive position Rx1, direction D2 using an x- and a y-aligned TX ULA vs the TX ULA shift and the RX antenna

For x-alignment of the TX antenna, the dominating DODs are in the interval $[-30°, 30°]$, whereas for y-alignment they are concentrated in the intervals $[-90°, -80°]$ and $[60°, 90°]$. The reason for different MIMO capacities for x- and y-aligned TX arrays is the nonlinear mapping of DODs on the phase factors of the corresponding array steering vectors as given by

$$\phi = \frac{2\pi d}{\lambda} \cdot \sin\left(\theta_{DOD}\right). \tag{4}$$

For fixed angular spread DODs departuring in broadside direction span a larger signal space than those departuring perpendicular to broadside direction. Therefore the first case leads to higher MIMO capacity. Exactly this happens in the measured scenario. From the transmitter, the paths propagate more or less only parallel to the corridor, whereas at the receiver the paths arrive from all directions. Therefore a rotation of the TX ULA has a great influence on the MIMO capacity but a rotation of the RX ULA does not.

5 Conclusion

Our measurements showed, that the MIMO capacity for constant average receive SNR is mainly independent on the receive position and direction within a single office. Nevertheless, two different receive positions using a specific receive direction show large capacity loss compared to all other positions and directions. Using simple beamforming methods, we showed that this is related to strong dominating components, whereas all other positions and directions show rather rich multipath scattering.

In contrast to the receive side, the transmit antenna alignment has a strong influence on the MIMO capacity. We showed that this can be related to dominant wave propagation parallel to the corridor. Therefore a perpendicular alignment of the TX antenna in respect to the dominant waves leads to significantly higher MIMO capacity than parallel alignment.

6 Acknowledgment

This work was supported by the European Union in form of a short term scientific mission within COST 273 ”Towards Mobile Broadband Multimedia Networks”. We would like to thank the EMC Testhouse Seibersdorf for giving us the possibility to make test measurements in their anechoic chamber. We would also like to thank Werner Weichselberger for fruitful discussions.

References

[1] D.P. McNamara, M.A. Beach, P.N. Fletcher, and P. Karlsson, “Capacity variation of indoor multiple-input multiple-output channels,” *Electronics Letters*, vol. 36, no. 24, pp. 2037–2038, November 2000.

[2] J. Wallace and M. Jensen, “Measured characteristics of the MIMO wireless channel,” in *VTC Fall 2001*, Atlantic City, N.J., USA, Oct. 2001.

[3] R. Thomä et al, “Identification of time-variant directional mobile radio channels,” *IEEE Trans. on Instrumentation and Measurement*, vol. 49, pp. 357–364, April 2000.

[4] G.J. Foschini and M.J. Gans, “On limits of wireless communications in a fading environment when using multiple antennas,” *Wireless Personal Communications*, vol. 6, no. 3, pp. 311–335, March 1998.

[5] H. Krim and M. Viberg, “Two decades of array signal processing research,” *IEEE Signal Processing Magazine*, vol. 13, pp. 67–94, July 1996.